Original Article

Inhibitory effect of *CUL1* on atherosclerosis through the p53 pathway

Xi Zhang[1#], Youwei Lu[1#], Wei Jiang[2], Qianhong Yang[1]

[1]Department of Geriatrics, Minhang Hospital, Fudan University, Shanghai, China; [2]Department of Neurosurgery, Minhang Hospital, Fudan University, Shanghai, China

Contributions: (I) Conception and design: Y Lu; (II) Administrative support: None; (III) Provision of study materials or patients: None; (IV) Collection and assembly of data: X Zhang; (V) Data analysis and interpretation: Q Yang, Y Lu; (VI) Manuscript writing: All authors; (VII) Final approval of manuscript: All authors.

[#]These authors contributed equally to this work.

Correspondence to: Qianhong Yang. Department of Geriatrics, Minhang Hospital, Fudan University, 170 Xinsong Road, Shanghai 201199, China. Email: yangqh73@163.com; Wei Jiang. Department of Neurosurgery, Minhang Hospital, Fudan University, Shanghai, China. Email: jiangwei_0821@fudan.edu.cn.

Background: Atherosclerosis (AS) is a serious chronic condition associated with cardiovascular and cerebrovascular diseases. Research on AS is currently lacking, and there is a need to increase research to improve the diagnosis, treatment, and prognosis of AS. Therefore, the aim of the present study was to explore the molecular mechanism and identify potential biomarkers in AS.

Methods: First, we downloaded the GSE28829 dataset and screened differentially expressed genes (DEGs). Then, DEGs were analyzed by functional enrichment analysis and protein-protein interaction (PPI) networks to determine hub genes. The key gene for AS was identified following the expression analysis of AS, clinical correlation with immune factors, the gene set enrichment analysis (GSEA) enrichment pathway, and receiver-operating characteristic curve analysis. In functional experiments, correlations between cullin 1 (*CUL1*), cytokines, and downstream targets in AS were investigated.

Results: We identified 595 upregulated and 391 downregulated DEGs enriched in neutrophil degranulation, the B-cell receptor signaling pathway, cell-matrix adhesion, and fatty acid degradation. Through PPI, we identified 7 hub genes for the expression analysis, immunoassay, and GSEA. Finally, *CUL1* was identified as the inhibitory gene in AS associated with immune factors, and was found to have a strong prognostic prediction ability. The results indicated that *CUL1* upregulated interleukin (IL)-6, IL-1β, and tumor necrosis factor-α concentrations, and weakened the cell proliferation of AS. It was also found that *CUL1* exerted its inhibitory function in AS by the p53 pathway.

Conclusions: The findings of the present study indicate that *CUL1* is a suppressing gene in AS, and has the potential to be a therapeutic and prognostic biomarker for AS.

Keywords: Atherosclerosis (AS); differentially expressed genes; cullin 1 (*CUL1*); immunoassay; p53 pathway

Submitted Aug 19, 2022. Accepted for publication Sep 15, 2022.
doi: 10.21037/atm-22-4372
View this article at: https://dx.doi.org/10.21037/atm-22-4372

Introduction

Atherosclerosis (AS) is a disease led by the residues deposited on the blood vessel wall for many years (1). It is the main pathological basis of cardiovascular diseases, such as cerebral infarction (2,3), and is associated with various complications during the onset of the AS, leading to shock and even death (4,5). There are no obvious features in its early stage, but chest tightness, dizziness, abdominal pain, lower limb gangrene, and other symptoms can occur later depending on the location of the lesion (6). Hypertension,

dyslipidemia, and smoking can increase the risk of AS (7-9). The age of AS onset is decreasing, and its incidence is increasing. The pathogenic factors of AS are very complex, often involving the arteries of the heart, brain, kidney, and other organs, which causes difficulty in the treatment process (10,11).

Microarrays, also known as oligonucleotide arrays, are a new molecular biology technique used to study how genes can interact and how a cell network can control a large number of genes at the same time (12,13). This technology has been widely used in exploring the molecular mechanism and clinical indicators of diseases, making it possible to develop the effective therapies (14-16). The Gene Expression Omnibus (GEO) database provides users with a free high-throughput gene expression online search platform (17). In the present study, we analyze the GEO database and a variety of bioinformatics analysis methods to study the mechanism of AS and explore new biomarkers for AS patients.

We applied various bioinformatics methods to analyze the GSE28829 dataset, including the Search Tool for the Retrieval of Interacting Genes (STRING) database, the Database for Annotation, Visualization and Integrated Discovery (DAVID) dataset, and Gene Set Enrichment Analysis (GSEA) to determine the key gene related to AS. Functional assays were then used to study the mechanism between *CUL1* (Cullin 1) and AS. The findings will help in finding biomarkers and therapeutic targets for AS. We present the following article in accordance with the MDAR reporting checklist (available at https://atm.amegroups.com/article/view/10.21037/atm-22-4372/rc).

Methods

Microarray data download

The GSE28829 dataset was downloaded from the GEO database. The dataset contained 29 samples, comprising 16 groups of advanced atherosclerotic plaque and 13 groups of early atherosclerotic plaque. We set the former as the experimental group and the latter as the control group to analyze the potential biological information of AS. The study was conducted in accordance with the Declaration of Helsinki (as revised in 2013).

Screening of differentially expressed genes

In this study, we used the limma package of the R software (MathSoft) to analyze and compare the differentially expressed genes (DEGs) in the experimental and control groups (18). We set the screening criteria for upregulation as fold change (FC) >1, and downregulation as FC <1, and both selections met P<0.001. A heatmap of the screening results was drawn using RStudio software.

Functional enrichment analysis of DEGs

The DAVID database (http://david.abcc.ncifcrf.gov/), established in 2003, provides systematic and thorough biological function annotation information for numerous gene or protein lists by integrating biological data and analytic methods. Gene Ontology (GO) provides a standard vocabulary for the attributes of gene products, including molecular function (MF), cellular component (CC), and biological process (BP) (19). The Kyoto Encyclopedia of Genes and Genomes (KEGG) is a database that examines gene functions in a systematic manner and connects genomic and functional data, including metabolic pathway databases, hierarchical classification databases, gene databases, and genome databases (20). In the present study, we performed functional annotation analysis on upregulated and downregulated DEGs by the DAVID database.

Protein-protein interaction network construction and module analysis

The STRING database is used for searching for connections between proteins in physics and function (21). First, we input 2 types of DEGs into the data to acquire a TSV format file. The protein-protein interaction (PPI) network was processed using Cytoscape software. To identify hub genes, we used molecular complex detection (MCODE) analysis to analyze upregulated and downregulated DEGs, and genes with top degree values in each group were identified as hub genes, integrin subunit beta 2 (*ITGB2*), integrin subunit alpha M (*ITGAM*), complement C3a receptor 1 (*C3AR1*), vesicle associated membrane protein 8 (*VAMP8*), S-phase kinase associated protein 1 (*SKP1*), *CUL1*, and ubiquitin C (*UBC*). The expression levels of 7 hub genes in the case group (AS) and the control group were investigated based on R software.

Correlation analysis between hub genes and immune factors

In this analysis, we used the dataset from the GEO

database; the download data format was MINiML. The heatmaps of the correlation between hub genes and chemokine, immunoinhibitor, immunostimulator, MHC (Major histocompatibility complex) molecule, and receptor were displayed using pheatmap in R software. Spearman's correlation analysis was used to describe correlations between hub genes and the above immune factors. P<0.05 was considered statistically significant.

GSEA and receiver-operating characteristic curve analysis of the 7 hub genes

GSEA is commonly used to detect the expression levels of 2 groups of samples that are significantly associated with specific biologically significant genomes (22). We uploaded the hub gene information to the GSEA website and used default parameters for analysis to study the biological functions of these genes. Furthermore, the survival receiver operating characteristic (ROC) curve package was used to assess the accuracy of AS prognosis when the hub gene was used as a predictive biomarker (23). According to the above results and previous research, *CUL1* was confirmed to be the key gene related to AS.

Cell culture

Human umbilical vein endothelial cells (HUVECs) were purchased from the Cell Bank of the Chinese Academy of Sciences (Shanghai, China). The cells were incubated in RPMI-1640 (Gibco, Grand Island, New York, USA) containing 10% fetal bovine serum (Gibco, USA), 50 mg/mL penicillin, and 100 mg/mL streptomycin (Solarbio, Beijing, China) in a humid environment at 37 ℃ and 5% CO_2.

Cell transfection

Over-NC and *CUL1* vector (over-*CUL1*) were purchased from Riobo and transfected into HUVECs using Lipofectamine 2000 (Thermo Fisher Scientific, Waltham, Massachusetts, USA) according to the manufacturer's instructions. The efficiency of transfection was detected by quantitative reverse transcription polymerase chain reaction (qRT-PCR). Pifithrin-α (PFT-α) is a commonly used p53 inhibitor that inhibits p53-dependent gene transcriptional activity, such as cell-cycle albumin. When there is an excess of oxidized low-density lipoprotein (oxLDL), the cholesterol it carries accumulates in the walls of arteries, causing AS over time. In the present study, oxLDL was applied to construct the AS model. The applied PFT-α and oxLDL were purchased from GenePharma (Shanghai, China).

qRT-PCR

Total RNAs were extracted from cells with TRIzol reagent (Invitrogen, Carlsbad, CA, USA) (24). We carried out reverse-transcription and real-time PCR assays using the PrimeScript RT reagent kit (Takara, Tokyo, Japan) and SYBR premix Ex Taq II kit (Takara, Japan). The $2^{-\Delta\Delta CT}$ method was used to measure the relative expressions of genes.

Cell Counting Kit-8

We used Cell Counting Kit-8 (CCK-8; Sigma, St. Louis, Missouri, USA) to verify cell viability. In total, 2×10^3 cells/well were seeded in a 96-well plate and cultured for 96 h (25). A total of 10 μL CCK-8 was added, and we evaluated the absorbance of each well at 450 nm. The growth curve used time as the horizontal axis and absorbance as the vertical axis.

Statistical analysis

To analyze the data, we used SPSS version 15.0 (SPSS, Chicago, IL, USA) and GraphPad Prism version 6.0 (GraphPad Software, La Jolla, CA, USA). To calculate significant differences, we used Student's *t*-test or one-way analysis of variance as appropriate. P<0.05 was considered statistically significant.

Results

Screening and functional analyses of DEGs

Using limma software, we screened 29 samples and obtained 986 DEGs, including 595 upregulated and 391 downregulated DEGs. The heatmap in *Figure 1A* shows the cluster distribution of these DEGs in 16 samples with advanced atherosclerotic plaque and 13 with early atherosclerotic plaque. In GO term, upregulated DEGs were enriched in neutrophil activation involved in immune response and neutrophil-mediated immunity (*Figure 1B*), and downregulated DEGs were enriched in cell-matrix adhesion and actin filament depolymerization (*Figure 1C*). Simultaneously, upregulated DEGs were enriched in the Leishmaniasis and B-cell receptor

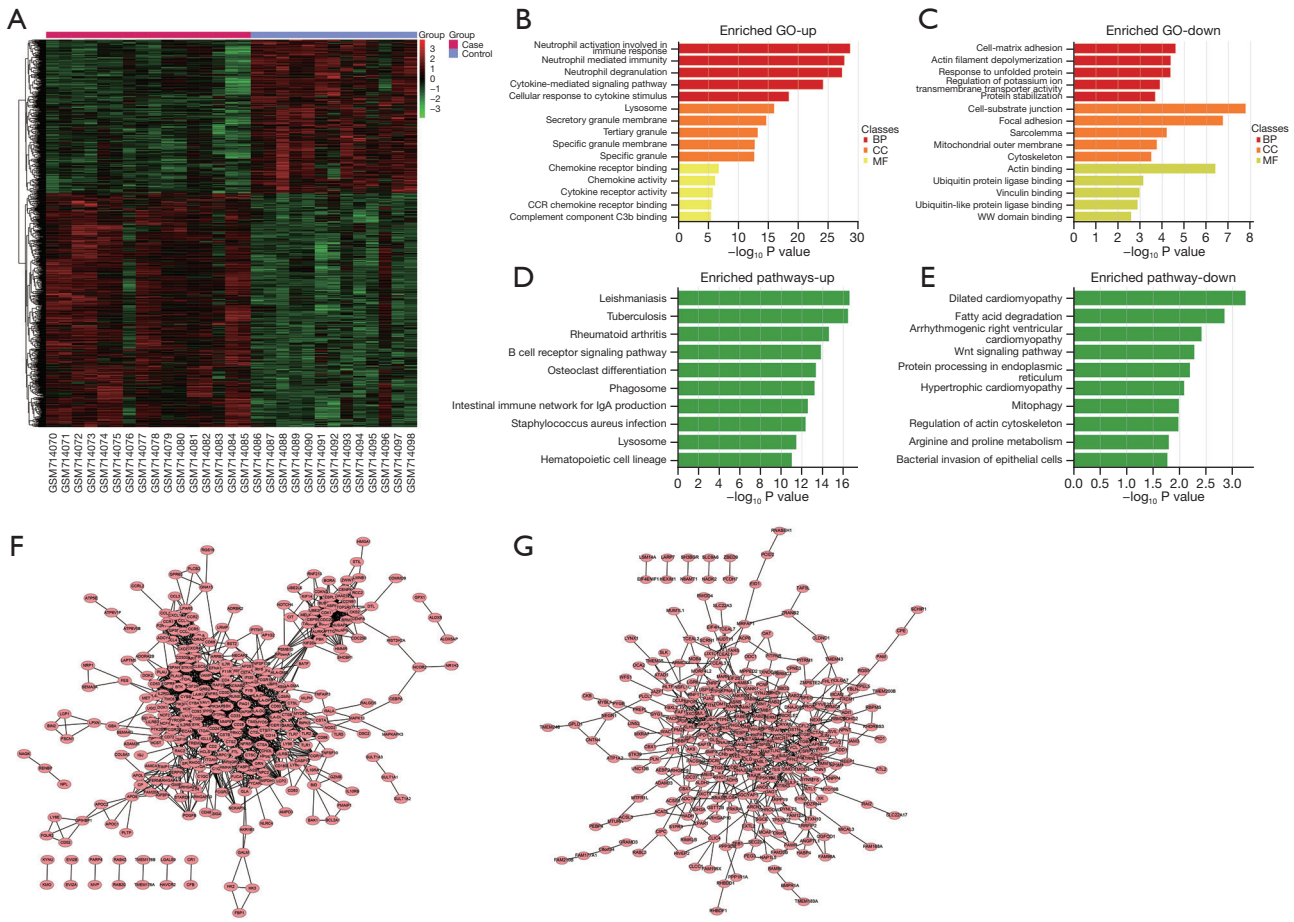

Figure 1 Visualization, functional enrichment, and PPI network analysis of DEGs. (A) Heatmap showing the expressions of DEGs in the case (red) and control groups (purple). (B,C) Gene Ontology enrichment analysis of upregulated and downregulated DEGs. (D,E) Enrichment pathways of upregulated and downregulated DEGs in Kyoto Encyclopedia of Genes and Genomes. (F,G) PPI network map of upregulated and downregulated DEGs. PPI, protein-protein interaction; DEGs, differentially expressed genes.

signaling pathways in KEGG (*Figure 1D*), and the top 10 KEGG pathways enriched by downregulated DEGs also included dilated cardiomyopathy and fatty acid degradation (*Figure 1E*). Based on the STRING network and Cytoscape software, we constructed upregulated PPI and downregulated PPI networks. The upregulated PPI network consisted of 311 nodes and 1,540 edges (*Figure 1F*), and the downregulated PPI network consisted of 293 nodes and 566 edges (*Figure 1G*).

Identification of the 7 hub genes

We then used the MCODE plug in to identify the degree values of DEGs, and identified the upregulated hub genes as *C3AR1* (degree =38), *ITGB2* (degree =37), *ITGAM* (degree =34), and *VAMP8* (degree =34, *Figure 2A*). *Figure 2B-2E* show the gene expression boxplots of the 4 upregulated hub genes. These boxplots indicated that the expression levels of the hub genes in the case group were higher than those in the control group (***P<0.001). In addition, the downregulated hub genes were *UBC* (degree =33), *SKP1* (degree =15), and *CUL1* (degree =14) (*Figure 3A*). The boxplots of these 3 downregulated hub genes are shown in *Figure 3B-3D*, and their expression levels in the case group were lower than those in the control group (**P<0.01).

Immunoassay of hub genes

Next, we explored the correlations of the 7 hub genes with immune factors using pheatmap. These immune

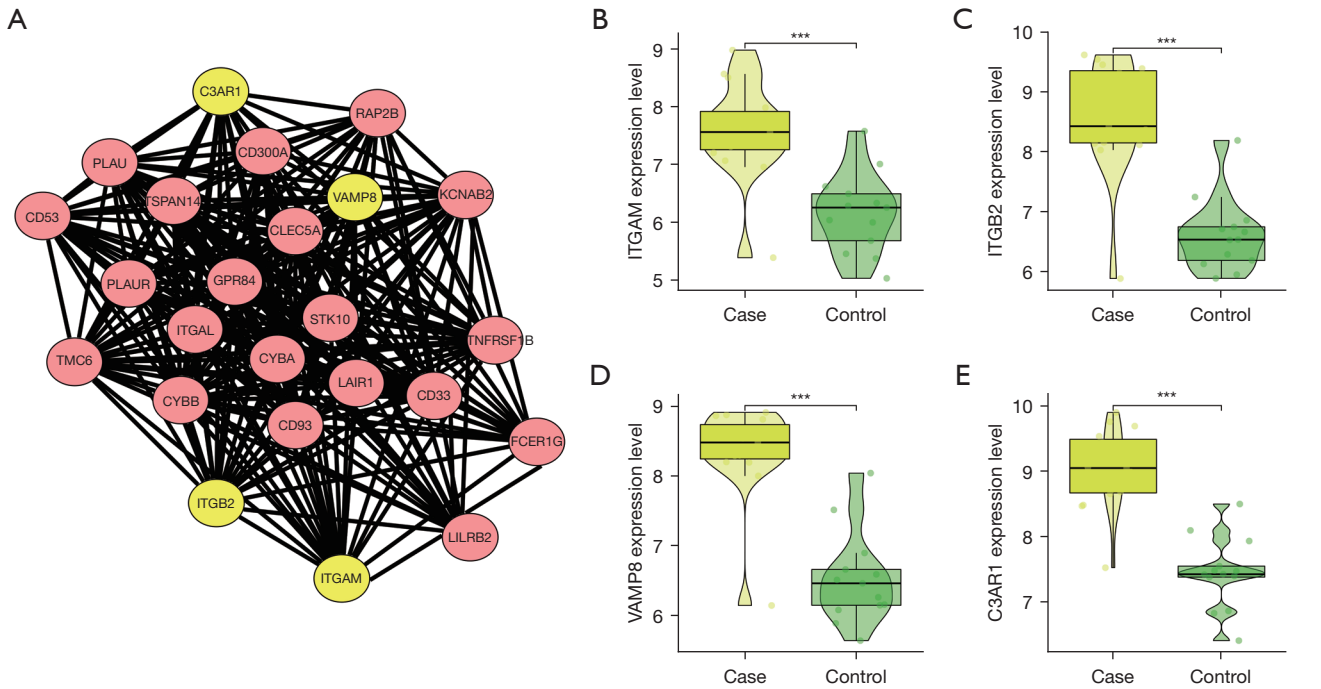

Figure 2 Screening of upregulated and downregulated hub genes. (A) Upregulated hub genes are shown in yellow. (B-E) Boxplots of *ITGAM*, *ITGB2*, *VAMP8*, and *C3AR1* expression analyses. ***P<0.001. *ITGAM*, integrin subunit alpha M; *ITGB2*, integrin subunit beta 2; *VAMP8*, vesicle associated membrane protein 8; *C3AR1*, complement C3a receptor 1.

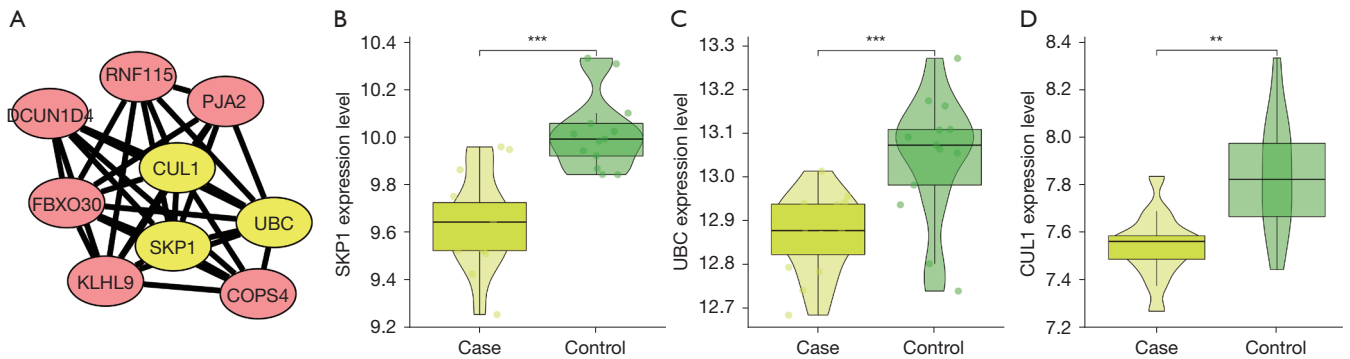

Figure 3 Screening of downregulated hub genes. (A) Downregulated hub genes are shown in yellow. (B-D) Boxplots of *SKP1*, *UBC*, *CUL1* expression analyses. **P<0.01, ***P<0.001. *SKP1*, S-phase kinase associated protein 1; *UBC*, ubiquitin C; *CUL1*, cullin 1.

factors included 5 categories in total, as follows: chemokine (*Figure 4A*), immunoinhibitor (*Figure 4B*), immunostimulator (*Figure 4C*), MHC molecule (*Figure 4D*) and receptor (*Figure 4E*). The results were shown by Spearman's correlation analysis. Blue indicated positive correlation and red indicated negative correlation (*P<0.05, **P<0.01). The 7 genes were found to be associated with these immune factors, especially chemokine and MHC molecule.

GSEA and prognostic value analysis of hub genes

To elucidate the biological functions of hub genes, we performed KEGG enrichment analysis on the 7 hub genes using GSEA software. The findings indicated that the up-regulated gene *ITGAM* was enriched in Systemic lupus erythematosus [*Figure 5A,5B*, area under the ROC curve (AUC) =0.903], *ITGB2* in Arachidonic acid metabolism (*Figure 5C,5D*, AUC =0.913), *VAMP8* in O glycan biosynthesis

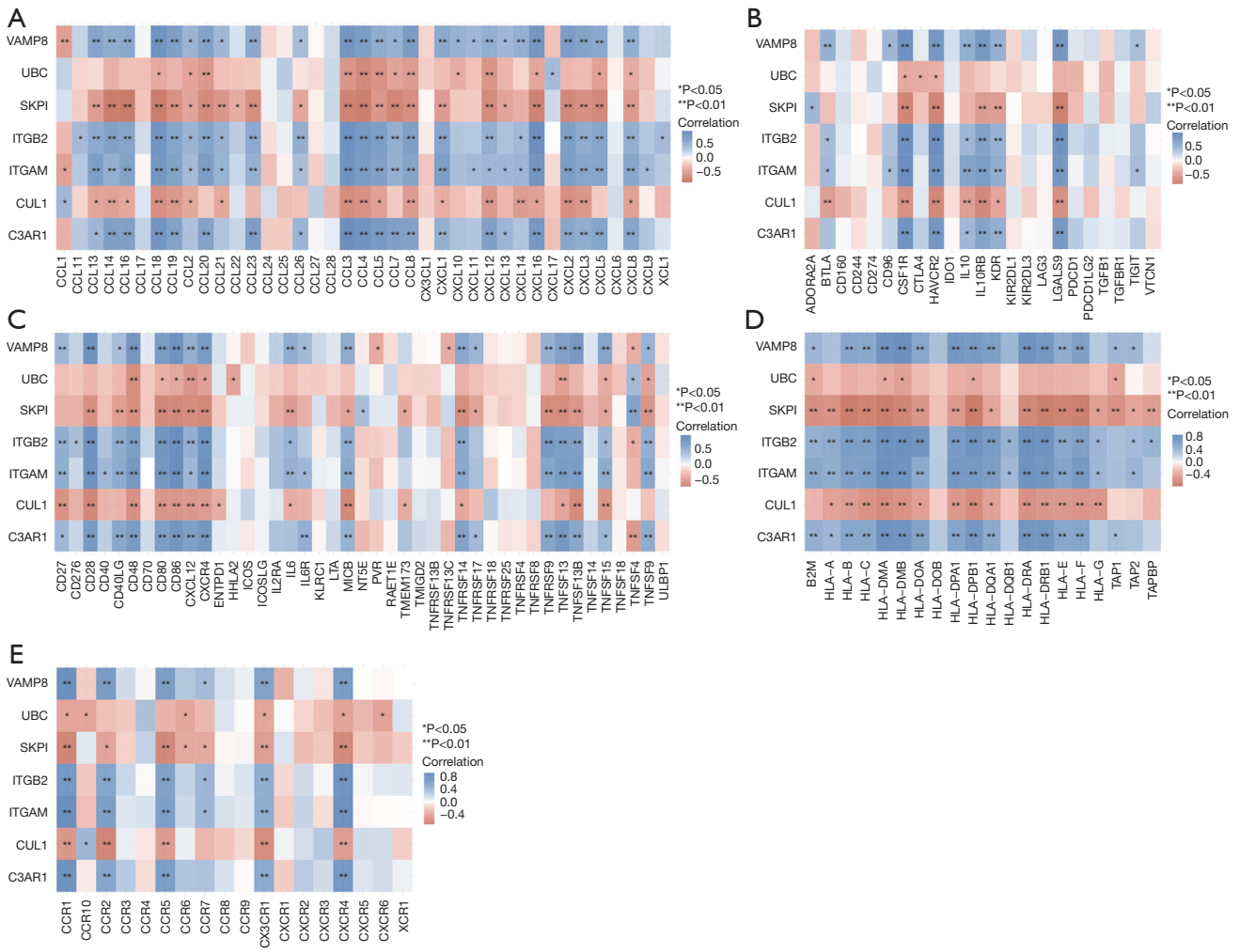

Figure 4 Heatmap of the correlation between the 7 hub genes and immune factors. Horizontal and vertical coordinates represent genes, and the different colors represent the correlation coefficient. Blue represents a positive correlation, and red represents a negative correlation. The darker the color, the stronger the correlation. *P<0.05, **P<0.01. Immune factors included (A) chemokine, (B) immunoinhibitor, (C) immunostimulator, (D) MHC molecule, (E) receptor. MHC, major histocompatibility complex.

(*Figure 5E,5F*, AUC =0.944), and *C3AR1* in Tryptophan metabolism (*Figure 5G,5H*, AUC =0.969). ROC curve of the upregulated hub genes (*ITGAM*, *ITGB2*, *VAMP8*, and *C3AR1*) indicated that their AUC values were all >0.7, which showed that they had a strong prognostic ability for AS. In addition, the downregulated hub gene *SKP1* was enriched in the Pentose phosphate pathway (*Figure 6A,6B*, AUC =0.938), *UBC* in Non-homologous end-joining (*Figure 6C,6D*, AUC =0.844), and *CUL* in Cell cycle (*Figure 6E,6F*, AUC =0.851). The AUC values of the downregulated hub genes (*SKP1*, *UBC*, and *CUL1*) were also >0.7, indicating that the downregulated hub genes also had a stronger prognostic predictive ability. These findings demonstrated that the 7 hub genes have the potential to be prognostic biomarkers for AS.

CUL1 could inhibit cell proliferation in AS

To determine an appropriate concentration of oxLDL in the AS model, we measured the relative expressions of *CUL1* with 50 and 100 μg/mL in HUVECs. The latter had better efficiency (*Figure 7A*). Therefore, 100 μg/mL was chosen for the next assays. Then, over-*CUL1* was transfected into HUVECs (*Figure 7B*). In CCK-8, it was found that oxLDL

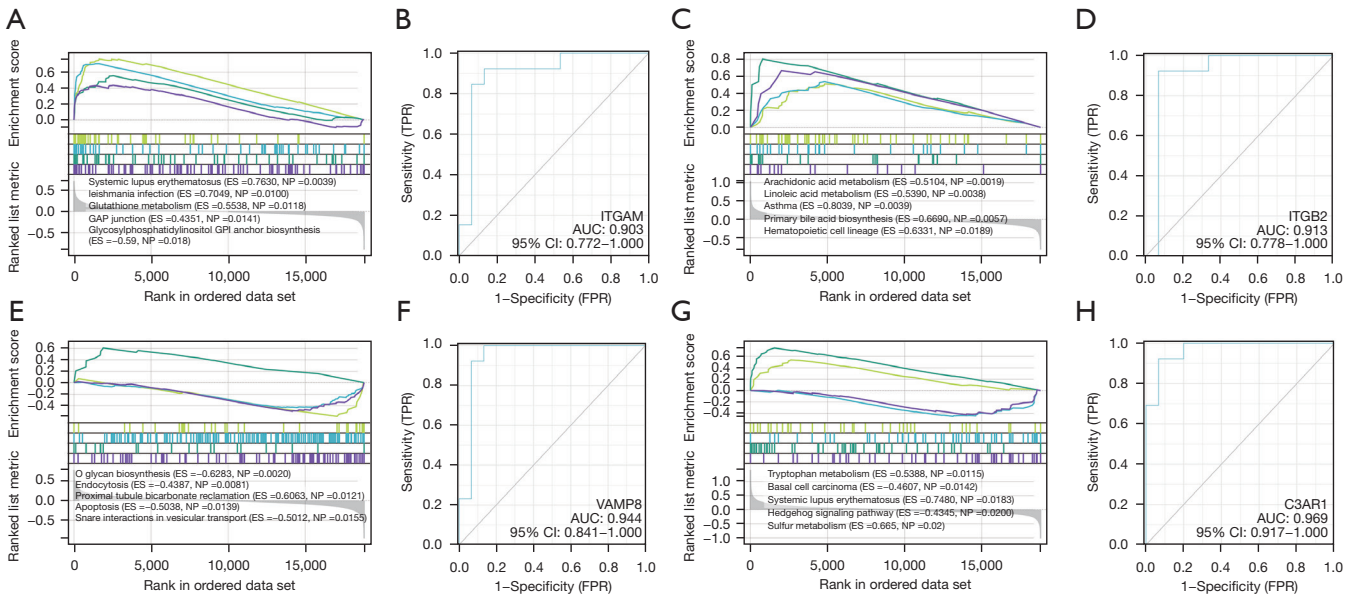

Figure 5 GSEA analysis and ROC curve analysis of upregulated hub genes. (A,B) Enrichment pathways and ROC curves of *ITGAM*. AUC =0.903. (C,D) Enrichment pathways and ROC curves of *ITGB2*. AUC =0.913. (E,F) Enrichment pathways and ROC curves of *VAMP8*. AUC =0.944. (G,H) Enrichment pathways and ROC curves of *C3AR1*. AUC =0.969. GSEA, gene set enrichment analysis; ROC, receiver-operating characteristic; AUC, area under the ROC curve; ES, Enrichment score; NP, NOM P-value; TPR, true positive rate; FPR, false positive rate.

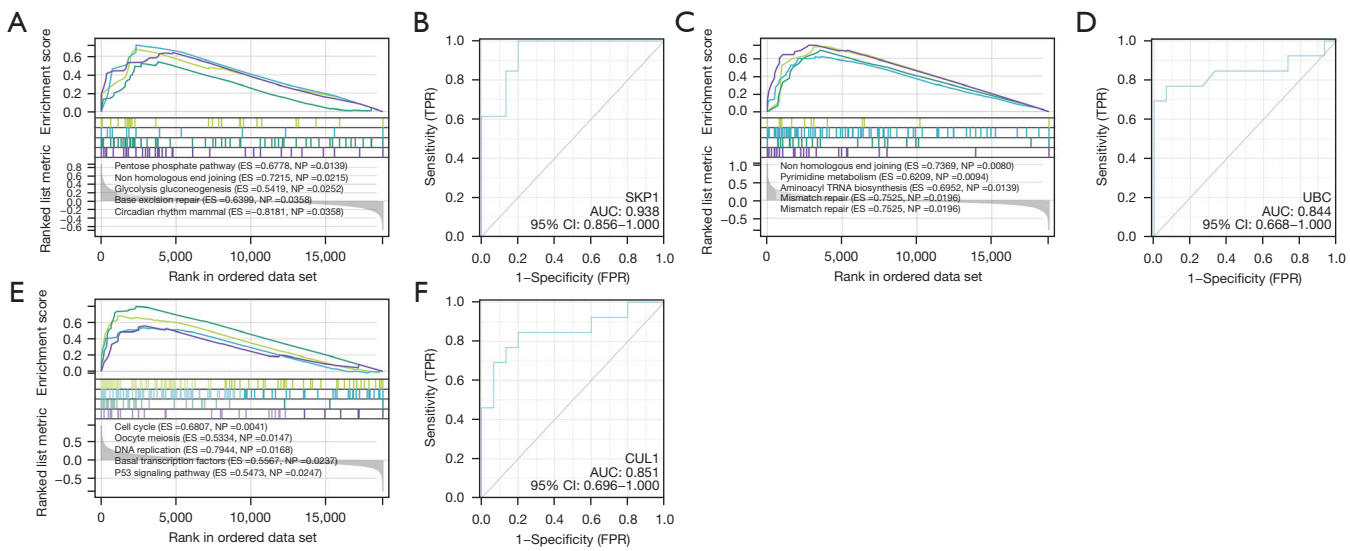

Figure 6 GSEA analysis and ROC curve analysis of downregulated hub genes. (A,B) Enrichment pathways and ROC curves of *SKP1*. AUC =0.938. (C,D) Enrichment pathways and ROC curves of *UBC*. AUC =0.844. (E,F) Enrichment pathways and ROC curves of *CUL1*. AUC =0.851. GSEA, gene set enrichment analysis; ROC, receiver-operating characteristic; AUC, area under the ROC curve; *CUL1*, cullin 1; ES, Enrichment score; NP, NOM P-value; TPR, true positive rate; FPR, false positive rate.

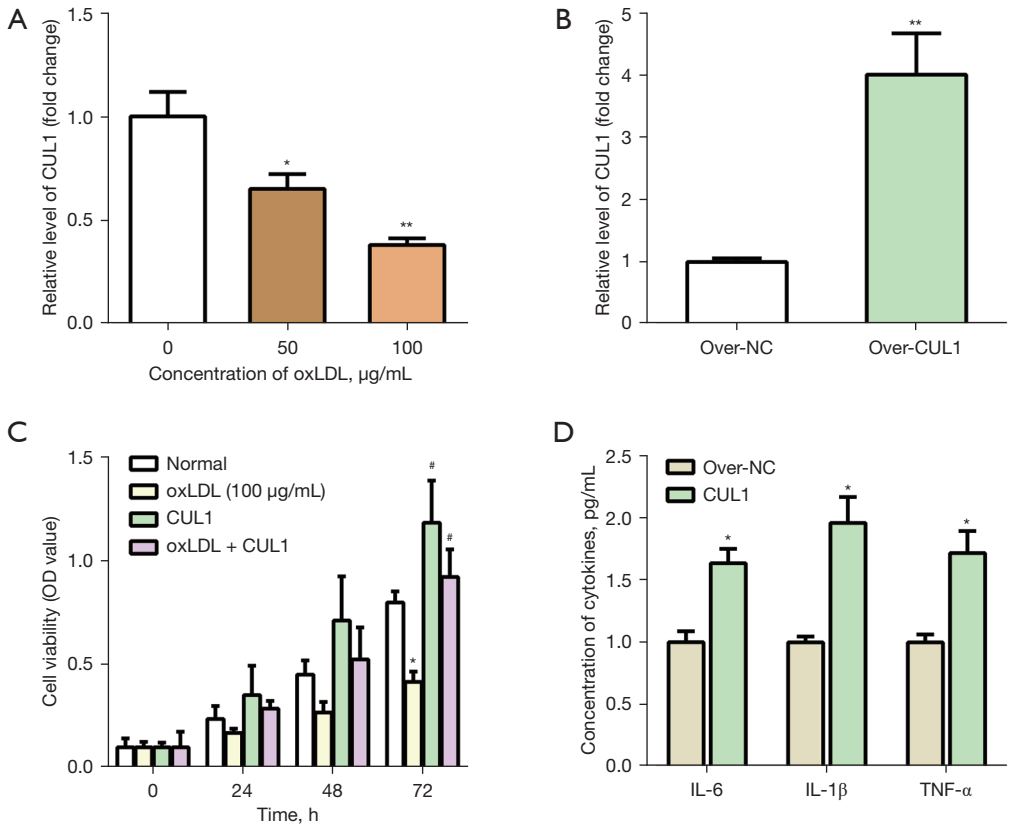

Figure 7 *CUL1* could inhibit cell proliferation in AS. (A) Relative expressions of *CUL1* with 50 and 100 μg/mL in HUVECs. (B) Over-*CUL1* was transfected into HUVECs. (C) *CUL1* could inhibit cell proliferation in AS. (D) Over-expressed *CUL1* could elevate the concentrations of cytokines. #P<0.05, compared with oxLDL group; *P<0.05, **P<0.01, compared with control group. *CUL1*, cullin 1; HUVECs, human umbilical vein endothelial cells; AS, atherosclerosis; oxLDL, oxidized low-density lipoprotein; NC, negative control; OD, optical density; IL, interleukin; TNF, tumor necrosis factor.

weakened cell viability compared with the normal group, *CUL1* promoted cell proliferation in HUVECs, and *CUL1* could inhibit cell proliferation in AS (*Figure 7C*). We also investigated the relationship between *CUL1* and cytokines. The data showed that over-expressed *CUL1* could elevate the concentrations of cytokines (*Figure 7D*).

CUL1 inhibits the progression of AS by the p53 pathway

Based on the GSEA results, we determined several candidate downstream targets of *CUL1* in AS, including the p53, *MDM*, *Bax*, caspase-9, caspase-3, and p21 pathways. Using qRT-PCR assays, the expressions of genes were detected in the following groups: normal, oxLDL (100 μg/mL), oxLDL + NC, oxLDL + *CUL1*, oxLDL + PFT-α, and oxLDL + PFT-α + *CUL1*. As shown in *Figure 8A*, the relative expression level of *CUL1* in those groups was detected. Then, the expressions of p53 (*Figure 8B*), MDM2 (*Figure 8C*), Bax (*Figure 8D*), caspase-9 (*Figure 8E*), caspase-3 (*Figure 8F*), and p21 (*Figure 8G*) were detected in the above groups. We found that in AS PFT-α had a negative relation with *CUL1*. Combined with the findings above, we supposed that p53 pathway might be the downstream target of *CUL1* in AS. As shown in *Figure 8H*, CCK-8 demonstrated that PFT-α could promote cell growth in AS, and *CUL1* had a positive association with p53.

Discussion

Apoptosis represents a major mechanism responsible for regulating the cellular structure of arterial walls during atherogenesis. Many environmental and endogenous factors can affect apoptosis through various signal transduction pathways or enzymatic systems. Abnormal apoptosis may occur in atherosclerosis, leading to a large accumulation of

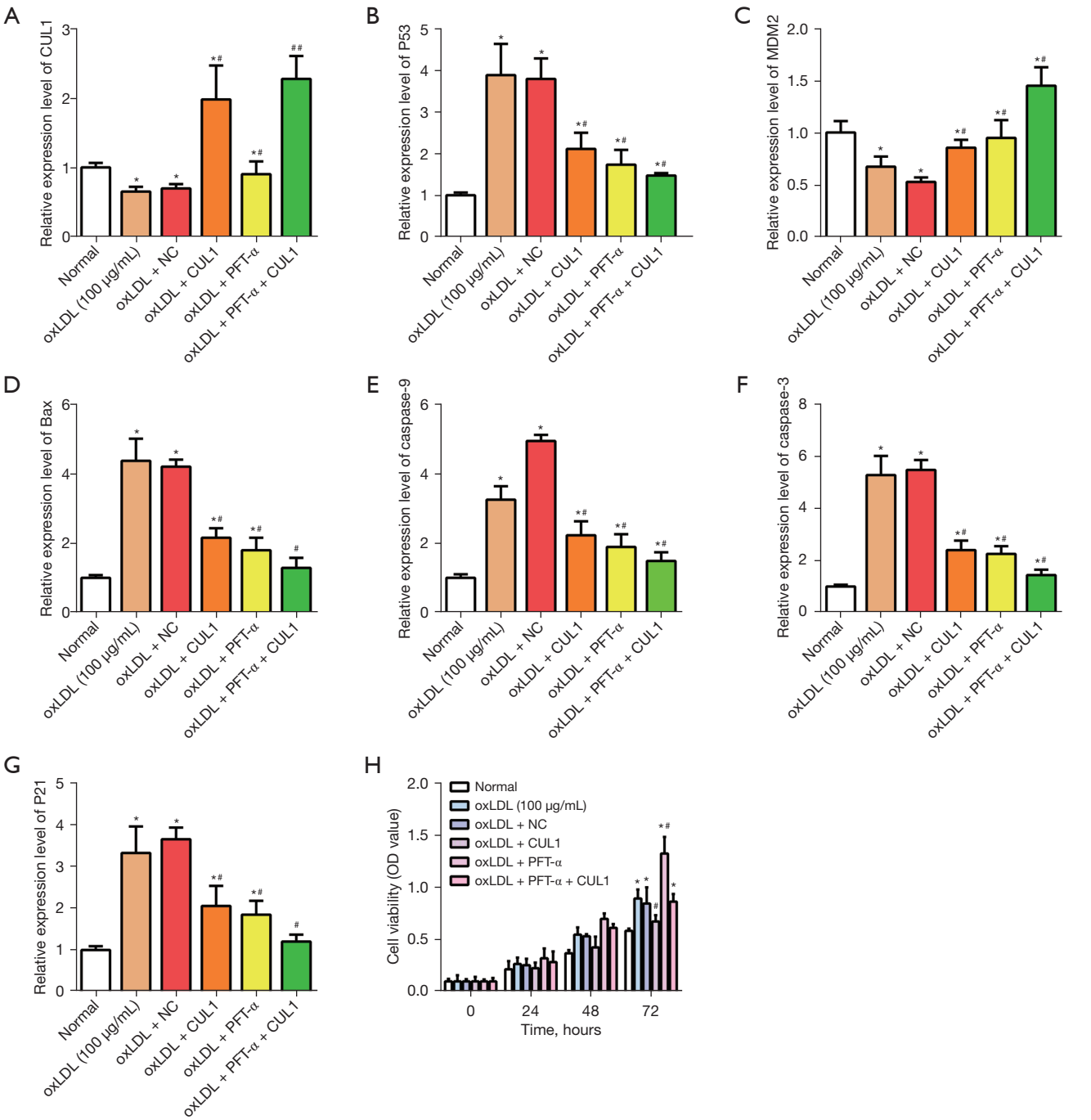

Figure 8 *CUL1* inhibits the progression of AS by the p53 pathway. (A) Relative expression levels of *CUL1* in each group were detected. (B-G) Expressions of the p53 (B), *MDM2* (C), *Bax* (D), caspase-9 (E), caspase-3 (F), and p21 (G) pathways in each group. (H) CCK-8 demonstrated that PFT-α could promote cell growth in AS. *P<0.05 compared with normal; $^{\#}$P<0.05, $^{\#\#}$P<0.01 compared with oxLDL. *CUL1*, cullin 1; AS, atherosclerosis; oxLDL, oxidized low-density lipoprotein; PET-α, pifithrin-α; NC, negative control; OD, optical density; CCK-8, cell counting kit-8.

intimal cells during the development of atherosclerosis. In advanced atherosclerotic plaques, especially during acute vascular syndromes, massive apoptosis of vascular cells may weaken the fibrous cap, promote thrombosis, and increase the risk of plaque rupture. Our study found that CUL1 can affect the proliferation and apoptosis of atherosclerosis through the expression of p53 signaling pathway proteins. Further elucidation of the molecular mechanism of vascular apoptosis may contribute to the clinical diagnosis and treatment of atherosclerosis.

Complications of AS are the leading cause of its morbidity and mortality (26). In aortic AS, aortic aneurysm is the main complication (27). In carotid artery and cerebral AS, long-term insufficient blood supply to the brain tissues can cause brain atrophy and intellectual disability. Cerebral hemorrhage and renal AS can cause renal atrophy and refractory hypertension (28). So far, no effective cure has been determined for AS. A deeper understanding molecular of AS will facilitate its diagnosis and treatment, and reduce the economic and social burden on AS patients.

In our research, we screened the GSE28829 dataset and identified 595 upregulated and 391 downregulated DEGs enriched in neutrophil degranulation, the B-cell receptor signaling pathway, cell-matrix adhesion, and fatty acid degradation, which were reported to be associated with heart diseases. Kawasaki *et al.* found that the increase in neutrophil degranulation affected a variety of biological processes that were altered in atrial fibrillation. In a separate cohort, patients with atrial fibrillation had an activated neutrophil in the left atrium, and neutrophil gene expression increased (29). Wang *et al.* found the B cell-receptor signaling pathway to be an important signaling pathway in controlling humoral immunity, and promote the formation of plasma cells (30). Other studies have shown that the B-cell receptor is a therapeutic target for chronic lymphocytic leukemia (31,32). Some researchers pointed out that the interaction between cells and cell-matrix adhesion and cell-extracellular matrix guides complex cell decisions in various physiological processes, including immune regulation, such as the passage of white blood cells through the blood and lymphatic system (33). Zhou *et al.* reported that fatty acid is the main inducer of endothelial cell apoptosis and inflammatory cytokines. Fatty acid results in endothelial dysfunction, causing macrophages, fibroblasts, and monocytes to adhere to the endothelium and migrate to endothelial cells. The migrated cells form a large number of lipid-laden foam cells, which eventually form atherosclerotic plaques (34). These terms and pathways might be potential therapeutic targets in AS treatment.

Next, we constructed PPI networks of upregulated and downregulated DEGs, and identified 4 upregulated and 3 downregulated hub genes as follows: *C3AR1*, *ITGB2*, *ITGAM*, *VAMP8*, *UBC*, *SKP1*, and *CUL1*. In their study, Zou *et al.* found that the expression of *C3AR1* in metastatic osteosarcoma was lower than that in non-metastatic osteosarcoma. Its overexpression inhibited the proliferation, migration, and invasion of osteosarcoma cells, and induced cell apoptosis (35). *C3AR1* is closely related to a variety of immune cells, such as macrophages (35). Blackburn *et al.* found that *ITGB2* is mainly expressed in the blood and encodes the integrin β chain (36). The *ITGB2* integrin β chain combines with a variety of α chains to form different integrin heterodimers. Integrin is a complete cell surface protein involved in cell adhesion and cell surface-mediated signal transmission (36). *CUL1* has been identified as a scaffold protein in the early development of chicken embryos (37). *CUL1* promotes the invasion of human trophoblast cells. Moreover, the abnormal expression of *CUL1* has been reported to be related to pre-eclampsia (38).

The expressions of the hub genes were detected in the AS group and control group through TCGA database. The results showed that upregulated hub genes were promotors, and downregulated hub genes were suppressors in AS progression. Their association with immune factors was also analyzed. The data demonstrated that the 7 hub genes were closely related to chemokine, immunoinhibitor, immunostimulator, MHC molecule, and receptor. These findings indicate that the 7 hub genes might be potential treatment targets for AS. Moreover, GSE28829 was clustered in systemic lupus erythematosus, arachidonic acid metabolism, tryptophan metabolism, the pentose phosphate pathway, non-homologous end-joining, and cell cycle. In ROC curves, all the hub genes showed good ability in AS prognosis prediction. Combined with all the analyses and previous research, *CUL1* was identified as the key gene for the functional experiments.

Through the functional experiment, the AS model was constructed by HUVECs with 100 μg/mL oxLDL. In the CCK-8 assays, we found that *CUL1* could inhibit the cell proliferation in AS, and its overexpression could increase the concentration of cytokines, which meant that *CUL1* was a suppressor gene in AS progression and had a positive relation with cytokines. To explore the downstream target of *CUL1* in AS, we started with the GSEA results of *CUL1*, namely cell cycle, oocyte meiosis, DNA replication, and basal transcription factors. Based on these, the candidate pathways were determined, including the p53, *MDM2*,

Bax, caspase-9, caspase-3 and p21 pathways. Through PCR assays, we inferred that p53 was the potential target, which was confirmed by CCK-8 assays. These results will assist in AS research.

There are certain limitations in our study, and there is a lack of corresponding *in vivo* experiments to further verify our conclusions. In the next study, we will further verify through animal real and clinical samples of atherosclerosis, and further clarify through *in vivo* experiments. CUL1 affects the progression of atherosclerosis.

Conclusions

In the present study, we identified 7 hub genes (*C3AR1*, *ITGB2*, *ITGAM*, *VAMP8*, *UBC*, *SKP1*, and *CUL1*) through multiple bioinformatics analyses that have the potential to be treatment targets and prognostic biomarkers in AS. In functional experiments, we found that *CUL1* could inhibit the cell proliferation of AS through the p53 pathway, which is of great significance for AS research. However, more studies are necessary to validate these findings.

Acknowledgments

Funding: None.

Footnote

Reporting Checklist: The authors have completed the MDAR reporting checklist. Available at https://atm.amegroups.com/article/view/10.21037/atm-22-4372/rc

Data Sharing Statement: Available at https://atm.amegroups.com/article/view/10.21037/atm-22-4372/dss

Conflicts of Interest: All authors have completed the ICMJE uniform disclosure form (available at https://atm.amegroups.com/article/view/10.21037/atm-22-4372/coif). The authors have no conflicts of interest to declare.

Ethical Statement: The authors are accountable for all aspects of the work in ensuring that questions related to the accuracy or integrity of any part of the work are appropriately investigated and resolved. The study was conducted in accordance with the Declaration of Helsinki (as revised in 2013).

References

1. Lusis AJ. Atherosclerosis. Nature 2000;407:233-41.
2. Zheng X. Research progress on the relationship between sphingomyelin signaling pathway and atherosclerosis. Chinese Journal of Arteriosclerosis 2019;27:87-92.
3. Xie S, Cheng W, Zhu J, et al. Research Progressonon the Mechanism of Atherosclerosis. World Journal of Complex Medicine 2016;2:85-90.
4. Carmeliet P, Hicklin DJ, Fang L, et al. Method of treating atherosclerosis and other inflammatory diseases: WO, EP1515707 A2[P]. 2005.
5. Shirai T, Hilhorst M, Harrison DG, et al. Macrophages in vascular inflammation--From atherosclerosis to vasculitis. Autoimmunity 2015;48:139-51.
6. Devanna N, Vanajakshi C, Bhaskar KV. Review on atherosclerosis. Pharmatutor 2013.
7. Vasconcelos LR, Lima FET, Magalhães FJ, et al. Risk factors identified in users subject to cardiac catheterization. Acta Scientiarum Health Science 2014;36:83-9.
8. Toregeani JF, Nassar CA, Toregeani KAM, et al. Periodontal disease and atherosclerosis. Jornal Vascular Brasileiro 2014;13:208-16.
9. Tridamayanti A, Wasyanto T. 5 Hypertension and smoking are still the leading risk factor for acute coronary syndrome in RSUD Moewardi. Journal of Hypertension 2019;37:e2.
10. Antelava NA, Pachkoriia KZ, Kezeli TD, et al., Major pathogenic links of atherosclerosis. Georgian Med News. 2005;(128):72-79.
11. Tomkin GH, Owens D. Investigational therapies for the treatment of atherosclerosis. Expert Opin Investig Drugs 2014;23:1411-21.
12. Singh-Gasson S, Green RD, Yue Y, et al. Maskless fabrication of light-directed oligonucleotide microarrays using a digital micromirror array. Nat Biotechnol 1999;17:974-8.
13. Vernon SD, Whistler T. Microarray technology for use in molecular epidemiology. Methods Mol Biol 2007;382:97-113.
14. Ojha S, Kostrzynska M. Examination of animal and

zoonotic pathogens using microarrays. Vet Res 2008;39:4.
15. Haley KJ, Lilly CM, Yang JH, et al. Overexpression of eotaxin and the CCR3 receptor in human atherosclerosis: using genomic technology to identify a potential novel pathway of vascular inflammation. Circulation 2000;102:2185-9.
16. Wang Z, Guo D, Yang B, et al. Integrated analysis of microarray data of atherosclerotic plaques: modulation of the ubiquitin-proteasome system. PLoS One 2014;9:e110288.
17. Liu H, MA W, Zheng W. GEO (Gene Expression Omnibus): High-throughput Gene Expression Database. Chinese Journal of Biochemistry & Molecular Biology 2007;23:236-44.
18. Cao J, Liu Z, Liu J, et al. Bioinformatics Analysis and Identification of Genes and Pathways in Ischemic Cardiomyopathy. Int J Gen Med 2021;14:5927-37.
19. Gaudet P, Logie C, Lovering RC, et al. Gene Ontology representation for transcription factor functions. Biochim Biophys Acta Gene Regul Mech 2021;1864:194752.
20. Gao S, Li F, Zhao M, et al. Identification of the Differentially Expressed Genes and Prognostic Associations in Single-Cell RNA Sequencing Data of Gastric Cancer. Available online: https://doi.org/10.21203/rs.3.rs-150872/v1
21. Szklarczyk D, Franceschini A, Kuhn M, et al. The STRING database in 2011: functional interaction networks of proteins, globally integrated and scored. Nucleic Acids Res 2011;39:D561-8.
22. Cai M, Hao Nguyen C, Mamitsuka H, et al. XGSEA: CROSS-species gene set enrichment analysis via domain adaptation. Brief Bioinform 2021;22:bbaa406.
23. Bai D, Feng H, Yang J, et al. Integrated analysis of coexpression and competitive endogenous RNA networks identified survival-related genes in gastrointestinal tumors. Available online: https://doi.org/10.21203/rs.3.rs-331336/v1
24. Pandey M, Chawla G. Total RNA isolation from Drosophila using TRIzol based reagent. Available online: https://www.researchgate.net/publication/350515148_Total_RNA_isolation_from_Drosophila_using_TRIzol_based_reagent.
25. Che H, Wang L, Ren Y, et al. CCK-8 cell viability assay. 2021(Preprint): p. 1481. Available online: https://bio-protocol.org/exchange/preprintdetail?type=3&id=1481
26. Majdalawieh AF, Yousef SM, Abu-Yousef IA. Thymoquinone, a major constituent in Nigella sativa seeds, is a potential preventative and treatment option for atherosclerosis. Eur J Pharmacol 2021;909:174420.
27. Woodrow P. Abdominal aortic aneurysms: clinical features, treatment and care. Nurs Stand 2011;25:50-7; quiz 58.
28. Savazzi GM, Cusmano F, Musini S. Cerebral imaging changes in patients with chronic renal failure treated conservatively or in hemodialysis. Nephron 2001;89:31-6.
29. Kawasaki M, Meulendijks ER, van den Berg NWE, et al. Neutrophil degranulation interconnects over-represented biological processes in atrial fibrillation. Sci Rep 2021;11:2972.
30. Wang XN, Ge X, Li J, et al. B cell receptor signaling pathway involved in benign lymphoepithelial lesions of the lacrimal gland. Int J Ophthalmol 2017;10:665-9.
31. Deglesne PA, Chevallier N, Letestu R, et al. Survival response to B-cell receptor ligation is restricted to progressive chronic lymphocytic leukemia cells irrespective of Zap70 expression. Cancer Res 2006;66:7158-66.
32. Packham G, Krysov S, Allen A, et al. The outcome of B-cell receptor signaling in chronic lymphocytic leukemia: proliferation or anergy. Haematologica 2014;99:1138-48.
33. Murai T, Kawashima H, Naor D. Editorial: Cell-Cell and Cell-Matrix Adhesion in Immunobiology and Cancer. Front Immunol 2020;10:3126.
34. Zhou H, Wang C. Cytoprotective Effects and Mechanisms of Δ-17 Fatty Acid Desaturase in Injured Human Umbilical Vein Endothelial Cells (HUVECs). Med Sci Monit 2017;23:1627-35.
35. Zou T, Liu W, Wang Z, et al. C3AR1 mRNA as a Potential Therapeutic Target Associates With Clinical Outcomes and Tumor Microenvironment in Osteosarcoma. Front Med (Lausanne) 2021;8:642615.
36. Blackburn NB, Marthick JR, Banks A, et al. Evaluating a CLL susceptibility variant in ITGB2 in families with multiple subtypes of hematological malignancies. Blood 2017;130:86-8.
37. Zhou W, Wei W, Sun Y. Genetically engineered mouse models for functional studies of SKP1-CUL1-F-box-protein (SCF) E3 ubiquitin ligases. Cell Res 2013;23:599-619.
38. Zhang Q, Chen Q, Lu X, et al. CUL1 promotes trophoblast cell invasion at the maternal-fetal interface. Cell Death Dis 2013;4:e502.

(English Language Editor: R. Scott)

Cite this article as: Zhang X, Lu Y, Jiang W, Yang Q. Inhibitory effect of *CUL1* on atherosclerosis through the p53 pathway. Ann Transl Med 2022;10(18):1008. doi: 10.21037/atm-22-4372

